Shape of the particulate beam attenuation spectrum and its inversion to obtain the shape of the particulate size distribution

Emmanuel Boss, Michael S. Twardowski, and Sean Herring

The link between the spectral shape of the beam attenuation spectrum and the shape of the particle size distribution (PSD) of oceanic particles is revisited to evaluate the extent to which one can be predicted from the other. Assuming a hyperbolic (power-law) PSD, $N(D) \propto D^{-\xi}$, past studies have found for an infinite distribution of nonabsorbing spheres with a constant index of refraction that the attenuation spectrum is hyperbolic and that the attenuation spectral slope γ is related to the PSD slope ξ by $\xi = \gamma + 3$. Here we add a correction to this model because of the finite size of the biggest particle in the population. This inversion model is given by $\xi = \gamma + 3 - 0.5 \exp(-6\gamma)$. In most oceanic observations $\xi > 3$, and the deviation between these two models is negligible. To test the robustness of this inversion, we perturbed its assumptions by allowing for populations of particles that are nonspherical, or absorbing, or with an index of refraction that changes with wavelength. We found the model to provide a good fit for the range of parameters most often encountered in the ocean. In addition, we found that the particulate attenuation spectrum, $c_p(\lambda)$, is well described by a hyperbolic relation to the wavelength $c_p \propto \lambda^{-\gamma}$ throughout the range of the investigated parameters, even when the inversion model does not apply. This implies that knowledge of the particulate attenuation at two visible wavelengths could provide, to a high degree of accuracy, the particulate attenuation at other wavelengths in the visible spectrum.

OCIS codes: 010.4450, 290.5850, 290.4020, 010.4450, 290.5850, 290.4020.

1. Introduction

Knowledge of particle size distributions (PSDs) is of fundamental importance in many areas of ocean science. The PSD can provide insight into the ecological dynamics of marine waters.[1] Information on PSD is of particular importance in the prediction of particulate sedimentation fluxes and sediment transport. Both particle settling rates and resuspension are dependent, to first order, on their size. Current methods for obtaining the PSD (e.g., Coulter counter analysis of a discrete sample) are labor intensive, require handling of water samples, and have the potential of altering the *in situ* PSD.[2–4] Because these methods require discrete sampling, they are impractical for obtaining distributions with high vertical resolution. However, laboratory techniques for obtaining PSD remain an invaluable tool and are unlikely to be completely replaced by *in situ* methods in the near future.

High-resolution (in space or in time) data used as input for sediment models currently come from a measurement of a single parameter (e.g., beam transmission or scattering in the back direction at a single wavelength), an indicator of particle concentration. With the advent of high-frequency *in situ* spectral attenuation meters (e.g., WET Labs ac-9),[5] measurements of spectral attenuation have become routine. Thus information on PSD could possibly also be obtained routinely. High-resolution PSD data are expected to enhance significantly the predictive capabilities of sediment-transport models, since both resuspension and settling are size dependent.[6] Several optical techniques exist that relate the PSD to particulate scattering.[7,8] Here we chose to evaluate a classical technique, which relates the spectral particulate beam attenuation, a relatively simple and robust measurement, to the PSD.

E. Boss (boss@oce.orst.edu) and S. Herring are with the College of Oceanic and Atmospheric Sciences, Oregon State University, Corvallis, Oregon 97331. M. S. Twardowski is with Western Environmental Technology Laboratories Incorporated, East Coast Branch, P. O. Box 468, Sauderstown, Rhode Island 02874-0468.

Received 20 February 2001; revised manuscript received 21 May 2001.

0003-6935/01/274885-09$15.00/0

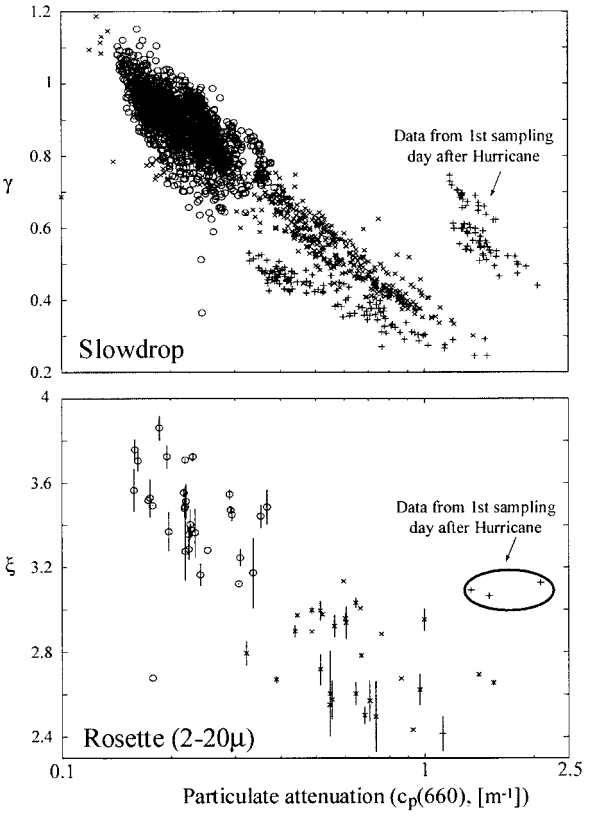

Fig. 1. (a). Particulate beam attenuation slope, γ, as function of beam attenuation at 660 nm obtained with a Slow Decent Rate Optical Profiler *in situ* and (b) PSD slope, ξ, as function of beam attenuation at 660 nm measured on water obtained from fitting of Coulter counter data on samples obtained by a Rosette platform. The measurements span two sampling periods (fall 1996, denoted by × and +, and spring 1997, denoted by ○) and are described and discussed in Boss *et al.*[12] The correlation of both attenuation slope and PSD slope with beam attenuation (and therefore with each other) is the primary motivation of the present study.

Links between the shape of the attenuation spectrum of particles and their size distribution have been derived theoretically[7,9–11] and observed empirically[1,7,12] (Fig. 1). A study by Voss[13] analyzed a large geographic data set of attenuation by particles plus dissolved substances and found its spectral shape to be quite constant; this study concluded that the attenuation spectra must be independent of the size distribution. However, a more recent study,[14] using a larger data set encompassing the full water column, found a different global spectrum than that of Voss. This study emphasized that the global spectrum that was found and the small variance around it are mostly due to the large dynamic range in the observations; in analysis of local data, large deviations from this global shape have been found. Indeed, concurrent observations of the size distribution of the PSD and attenuation spectrum at one location included in the above study[14] show that in the bottom boundary layer large changes in PSD and attenuation spectrum are present and well correlated[12] (Fig. 1).

A. Theoretical Background

PSDs are often described by a simple two-parameter (N_0, ξ) differential power-law function

$$N(D) = \begin{matrix} 0 & D > D_{\max} & D < D_{\min} \\ N_0(D/D_0)^{-\xi} & D_{\max} > D > D_{\min} & \end{matrix}, \quad (1)$$

where $N(D)$ is the number of particles with diameters between D and $D + \mathrm{d}D$ divided by $\mathrm{d}D$, D_0 is a reference diameter for which the number concentration is N_0, and ξ is the differential slope parameter. The distribution is, in fact, a four-parameter distribution, since $D_{\min}$ and $D_{\max}$, the minimum and maximum particle size, define it as well. When fitted to measured particle populations, $D_{\min}$ is often fixed by the detection limit of the sizing instrument (generally 0.5–1.0 μm for a Coulter counter). The parameter $D_{\max}$ will be fixed by either the environment (in the ocean there is often a 2-mm cutoff,[15] most likely due to turbulence) or an instrumental orifice. The mean particle size for such a PSD is readily calculated:

$$\overline{D} \equiv \frac{\int_{D_{\min}}^{D_{\max}} DN(D)\mathrm{d}D}{\int_{D_{\min}}^{D_{\max}} N(D)\mathrm{d}D} = \left(\frac{1-\xi}{2-\xi}\right) \times \left(\frac{D_{\max}^{2-\xi} - D_{\min}^{2-\xi}}{D_{\max}^{1-\xi} - D_{\min}^{1-\xi}}\right) \overset{D_{\min} \ll D_{\max}}{\approx} \left(\frac{1-\xi}{2-\xi}\right) D_{\min}. \quad (2)$$

For a hyperbolic PSD with $\xi > 2$, as observed in the ocean, the mean particle size increases with decreasing ξ .

The applicability of Eq. (1) to PSDs in the ocean has been shown in many studies[15,16] and used in many theoretical studies.[10,17,18] Typically, $2.5 < \xi < 5$. Although in many cases other functions with more free parameters have been found to better fit the observed PSD,[7,19,20] Eq. (1) is still the most widely used model to describe marine PSDs. McCave[21] has shown that particle number data can, in nearly all cases, be fitted by an equation such as Eq. (1) over a large part of the measured range. Although we recognize that Eq. (1) is an ideal fit to the true PSD in only rare cases, we believe it is reasonable that PSD approximations with a simple power-law model will be highly informative nonetheless. A limitation of this size distribution is that it is discontinuous and has a tendency to overestimate the slope of the smallest particles in observations.[1,7] It is important to emphasize, however, that there is little data available on the PSD below 1 μm. Despite these apparent limitations, Eq. (1) was chosen as the model in this analysis, recognizing that Eq. (1) may not be the ideal descriptor of the PSD, but a consensus on an ideal PSD model has not been reached; given the degrees of freedom in the spectral attenuation measurement in the visible part of the spectrum (given its simple shape), it is not likely that it can be inverted

to anything more descriptive than a two-parameter-fit PSD or the mean particle size. Nonetheless, this approximation is expected to be of significant value for many applications, including interpretation of *in situ* data and data assimilation into sedimentation models.

Theoretical analysis based on Mie theory and its approximations[9–11] for nonabsorbing particles, with constant index of refraction, assuming a PSD of the type of Eq. (1), and with diameters spanning from $D_{\min} = 0$ to $D_{\max} = \infty$, have demonstrated that the particulate attenuation spectrum is described well by

$$c_p(\lambda) = A\lambda^{-\gamma}. \tag{3}$$

In addition, the PSD and $c_p(\lambda)$ are linked according to the simple relationship

$$\xi = \gamma + 3. \tag{4}$$

Equation (4) provides an inversion from the spectral shape of the particulate beam attenuation [Eq. (3)] to the shape of the PSD [Eq. (1) or (2)]. Volz and others[9–11] pointed out that the applicability of Eqs. (2) and (3) depends on the limits of the integral

$$c_p = \int_{D_{\min}}^{D_{\max}} C_{\text{ext}}(D)N(D)\mathrm{d}D, \tag{5}$$

where C_{ext} is the attenuation cross section, i.e., the attenuation of a single particle with diameter D. When the limits $D_{\min}$ and $D_{\max}$ are 0 and infinity, respectively, Eqs. (3) and (4) are exact. However, as the limits of integration change, departure from Eqs. (2) and (3) are to be expected, especially for low values of ξ, owing to the monotonically increasing behavior of C_{ext} with D. Often the equations are cast in terms of a nondimensional size parameter, $\alpha = \pi D/\lambda$, because of the invariance of the attenuation cross section to this parameter (for indices of refraction near unity[22]). The problem arises when the PSD has finite width, because a constant limit in D does not translate into a constant limit in the size parameter, since the wavelength is allowed to vary.[10] In practice, with measurements of the beam attenuation, $D_{\min}$ is often fixed by a physical filter used to define the particulate phase in contrast to the dissolved phase (most often varies between 0.2 and 0.7 μm; since the dissolved fraction consists of the absorbing colored dissolved organic matter, it needs to be separated from the particulate fraction). The upper limit, $D_{\max}$, is fixed by the environment, the physical size of the beam, instrument orifice, or a data-smoothing algorithm designed to filter the rare, larger particles. Although Eq. (3) is nearly exact for finite, though wide, constant limits in the size parameter,[11] this is not the case with realistic limits in D, as shown below.

B. Scope of Present Study

In the present study we quantify the limits of applicability of the hyperbolic shape to the particulate attenuation [Eq. (3)] and the applicability of the classical inversion to obtain the PSD shape from the shape of the particulate attenuation [Eq. (4)].

Except for in the limited, yet insightful, analysis of Morel,[10] the limits for the applicability of Eqs. (3) and (4) have not been systematically addressed. In Fig. 1 we present data obtained during the coastal mixing and optics experiment, which relates the attenuation spectral slope, γ, with the PSD slope, ξ, as measured by a Coulter counter. These data suggest that the two are well correlated, though the difference between ξ and γ is not 3 [Eq. (4)]. As a matter of fact, the difference decreases with γ, and $\gamma > 0$, despite observations of $\xi < 3$. The differences between the classical inversion [Eq. (4)] and the observations prompted us to revisit the theory underlying the inversion. We perturb several assumptions of the classical theory including finite bounds for the particulate size, absorbing particles, the effects of a spectrally varying particulate index of refraction, and nonsphericity, all of which are consistent with marine particles. In addition, we study the general applicability of Eq. (3) as a fit to spectral c_p. We have found it to provide a good fit to field data[12] and are investigating its theoretical application here.

2. Materials and Methods

Mie theory was used to compute the optical properties of particles. The two main assumptions of Mie theory are that the particles are homogeneous and that they are spherical. Mie theory has been used successfully to predict various optical properties of oceanic particles.[7,10,23] A code provided in the appendix A of Bohren and Huffman[24] and translated into the operating language of MATLAB was used to carry out the computation.

Calculations of spectral attenuation were performed for eight equally spaced wavelengths in the range $440 \le \lambda \le 650$ (wavelengths are given in vacuum), with the real part of the index of refraction varying between $1.02 \le n \le 1.2$ and the imaginary part of the index of refraction between $0 \le n' \le 0.01$. Diameters were varied from $D_{\min}$ to $D_{\max}$ (see below) with the spacing increasing logarithmically. Values of ξ were varied between 2.5 and 5 to reflect the range of variability observed in the oceans.

We used a Levenberg–Marquardt nonlinear minimization[25] to fit Eq. (3) to the computed spectral particulate attenuation. We used two measures of goodness of fit: (i) the maximum percentage deviation between modeled data and the fit of Eq. (3) and (ii) the average root-mean-squared (rms) difference between modeled data and fit divided by the averaged attenuation. The two measures represent the worst possible percentage error at a given wavelength and the likely percentage error, respectively.

For the calculations of attenuation by nonspherical particles we used the approximation of Fournier and Evans.[26,27] Comparing this approximation with results from the more rigorous but size-restricted T-matrix method,[28,29] we found excellent agreement as did Evans and Fournier.[27] We calculate the spectral attenuation for two nonspherical particles oblate

spheroids with an axis ratio of 3 and prolate spheroids with an axis ratio of 1/3.

3. Results

A. Nonabsorbing Particles

The shape of the attenuation spectrum and the dependency γ on ξ were first evaluated for populations of nonabsorbing particles. Size limits for the populations were varied between $D_{min} = 0.01$ μm and $D_{max} = 300$ μm. The values of D_{min} and D_{max} were chosen such that halving or doubling them (respectively) had a relatively small effect on the results. For the range of parameters $1.02 \le n \le 1.2$ and $2.5 \le \xi \le 5$ it was found that the maximum departure of the modeled $c_p(\lambda)$ data from a hyperbolic function of the wavelength [Eq. (3)] was 0.14%.

A nonlinear fit to the dependence of ξ on γ [for various n, and assuming that the deviation from Eq. (4) is exponential] is given by

$$\xi = \gamma + 3 - 0.5 \exp(-6\gamma). \quad (6)$$

The maximum deviation between the input ξ and that computed from Eq. (6), for all input values of n and ξ, was 0.16 for $\xi = 2.5$ and $n = 1.02$. This inversion performs worst for small ξ, because $d\xi/d\gamma$ increases with decreasing ξ, as the beam attenuation becomes nearly constant as function of wavelength. Note that the difference between Eqs. (6) and (4) is less than 0.15 for $\gamma > 0.2$, and thus the two inversions, in most cases, are not significantly different from each other. Since ξ based on Eq. (4) will always be more biased compared with that based on Eq. (6), Eq. (6) will be used henceforth as our reference inversion equation as we vary certain parameters of the particles.

For the same parameters, but keeping the Mie size parameters α_{min} and α_{max} constant (rather than D_{min} and D_{max}), the results are in excellent agreement with Eq. (4) for the full range of ξ tested. Although α_{min} and α_{max} have been assumed to be constant in some studies in which Eq. (4) has been derived and used,[11,30] it is not a valid assumption here, since α will vary with wavelength for a fixed maximum and minimum particle size.

B. Effects Due to D_{min} and D_{max}

As discussed in Section 1, departures from Eq. (4) or (6) depend on the sizes of the smallest and the biggest particles. Small particles have a relatively larger contribution for large ξ, whereas large particles contribute more at small ξ. To investigate this effect, we varied each limit of the integral [Eq. (5)] while keeping the other limit constant (Fig. 2). We computed γ for each particulate attenuation spectrum (for each input n and ξ) and computed the difference between the input PSD slope and that based on Eq. (6) (Fig. 2) for two limiting indices of refraction (1.02 and 1.2).

Clearly, large differences are observed between the input PSD slope and that computed on the basis of Eq. (6) when the particles below 0.2 μm are neglected. We chose a departure of 0.15 in ξ from Eq. (6) as an arbitrary tolerance for applicability of Eq. (6). On the basis of this criterion, and given the assumptions of the model, $D_{min} < 0.2$ μm and $D_{max} > 150$ μm are needed for Eq. (6) to be applicable for populations with a single index of refraction with a value between 1.02 and 1.2 and with ranges of PSD slopes of the order of $3 \le \xi \le 4.5$ (Fig. 3). Equation (6) has a broader range of applicability for particles with intermediate indices of refraction (not shown).

Although Eq. (6) did not approximate ξ well for all D_{min} and D_{max}, Eq. (3) still provided a good fit for the attenuation. The maximum relative deviation from Eq. (3) was 2% (rms 0.007%).

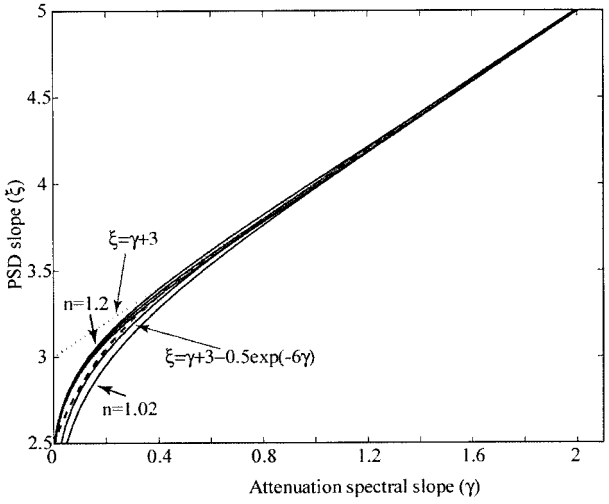

Fig. 2. PSD slope, ξ, as function of the attenuation spectrum (γ) of nonabsorbing particle populations. The modeled populations have slopes $5 \ge \xi \ge 2.5$, indices of refraction $n = 1.02$, 1.05, 1.09, 1.15, and 1.2, and a size range $300 \ge D \ge 0.01$ μm. The dashed and the dotted curves represent the $\xi - \gamma$ relationships of Eqs. (4) and (6), respectively. Maximum deviation of the attenuation spectrum from a hyperbolic model [Eq. (3)] is 0.35% (mean rms 0.0003%).

C. Particles with Index of Refraction that Varies with Wavelength

In addition to the assumptions associated with Mie theory (sphericity and homogeneity of the particles), we have also assumed that the real part of the index of refraction of the particles does not depend on wavelength. Although Eqs. (4) and (6) do not depend explicitly on the index of refraction of the particles, the magnitude of the particulate attenuation, $c_p(\lambda)$, is a strong function of the index of refraction, and thus we may expect variations in the fit of Eq. (2). For nonabsorbing particles the variations in index of refraction in the visible wavelengths are small and are expected to follow the theory of normal dispersion.[22] Normal dispersion refers to the decrease, for weakly absorbing particles, of the refractive index as a function of wavelength. This decrease can be shown to

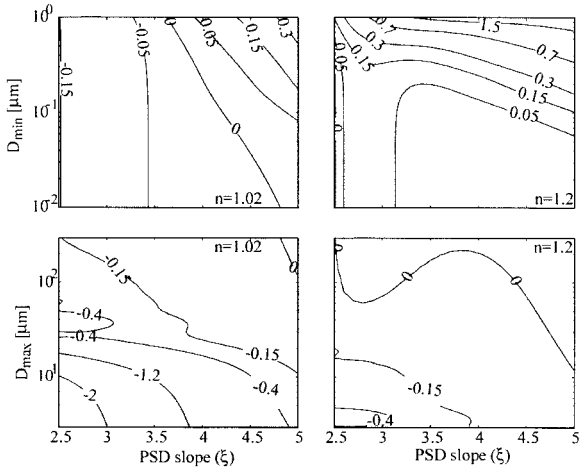

Fig. 3. Effect of changing the population size limits. Difference between input and modeled [Eq. (6)] PSD slope (ξ) as a function of the size of the smallest particles (D_{min}, upper two panels) and largest particles (D_{max}, lower two panels) for populations with different ξ. Left-hand panels are for nonabsorbing particles with index of refraction $n = 1.02$, and right-hand panels are for $n = 1.2$. Negative values indicate that the model [Eq. (5)] overestimates the population's PSD slope. Maximum deviation of the attenuation spectrum from a hyperbolic model [Eq. (3)] with varying D_{max} was 2.1% (mean rms 0.01%) and when varying D_{min} was 0.23% (mean rms 0.007%).

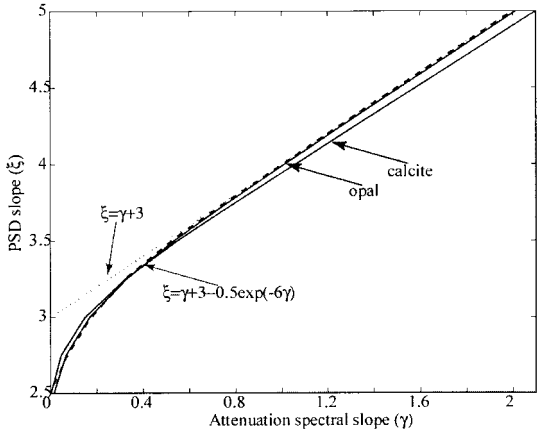

Fig. 4. Effect of spectrally varying refractive index. PSD slope, ξ, as function of the attenuation spectrum (γ) of calcite and opal particle populations with different size distribution slopes (ξ) with a constant size range $300 \geq D \geq 0.01\mu m$. The spectrally variable index of refraction was computed from Eq. (7) with the parameters in the text. The dashed and the dotted curves are the proposed ξ–γ relationships based on Eq. (4) and Eq. (6), respectively. Maximum deviation of the attenuation spectrum from a hyperbolic model [Eq. (3)] for calcite was 0.3% (rms 0.006%) and for opal was 0.06% (rms 0.0004%).

obey an equation of the form (see Aas[31], and references therein)

$$n(\lambda) = P' + Q'/\lambda^2, \tag{7}$$

where P' and Q' are substance dependent. As examples of nonabsorbing material from which some oceanic particles are composed we chose (from Aas,[31] Table 9) a population of calcite particles ($P' = 1.197$, $Q' = 1720\ nm^2$) and opal particles ($P' = 1.073$, $Q' = 90\ nm^2$) and evaluated the effects of variable n on the fit (Fig. 4). The fit [Eq. (6)] is still found to be good (maximum difference in ξ between the model and Mie for calcite was 0.1). Again, Eq. (3) provided a good model for the attenuation spectrum with maximum deviation of 0.2% for population of opal and calcite particles.

D. Absorbing Particles

The theory we are revisiting here was derived for nonabsorbing particles. Since many types of oceanic particles absorb light, it is of interest to know the limit of applicability of Eqs. (3) and (6) for absorbing particles. To evaluate the effect of absorption, we added a spectrally constant imaginary part to the index of refraction and evaluated the departure of γ from Eq. (6) (Fig. 5). For particles with a low refractive index, Eq. (6) is valid up to $4 \geq \xi$. For particles with higher indices of refraction, Eq. (6) applies for a larger range of PSD slopes, namely, $4.5 \geq \xi$. The departure from Eq. (6) also increases with absorption (increase in the imaginary part of the index of refraction).

Absorbing particles exhibit, in addition to normal dispersion [Eq. (7)], anomalous dispersion, in which the real part of the index of refraction is modified by the value of the imaginary part of the index of refraction.[22,31] Variations of n due to anomalous dispersion in algal cells are expected to be of the order of 0.001–0.005, and in extreme cases, 0.008. Aas[31] concludes that the anomalous dispersion of the refractive index will probably influence only the scattering properties of small phytoplankton in the vicinity of strong absorption bands. This is consistent with Fig. 5, where we found absorption to affect mostly results in populations with large ξ (relatively more small particles). Experimenting with phytoplankton-like, wavelength-dependent indices of refraction (e.g., Stramski *et al.*[32]) we found (not shown) that although the results were very similar to those of populations with constant real and imagi-

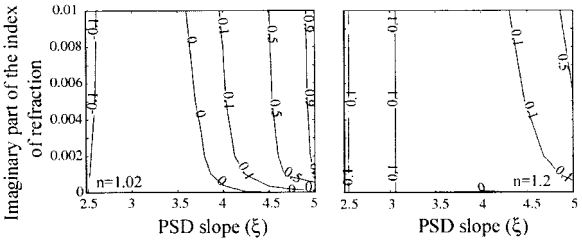

Fig. 5. Effect of absorption. Difference between input and modeled [Eq. (6)] PSD slope (ξ) as a function of the magnitude of the imaginary part of the index of refraction for populations with different ξ. Left-hand panel is for absorbing particles with index of refraction $n = 1.02$, and right-hand panel is for $n = 1.2$. Negative values indicate that the model [Eq. (6)] overestimates the population's PSD slope. Maximum deviation of the attenuation spectrum from a hyperbolic model [Eq. (3)] was 0.26% (rms 0.003%).

nary parts of the refractive index, departure from the model [Eq. (6)] increased, yet Eq. (6) was still applicable for $\xi < 4$.

E. Nonspherical Particles

Most oceanic particles are not spherical.[33] Since Mie theory assumes sphericity, it is important to see whether the relation between the shapes of the PSD and attenuation spectrum changes for such particles. Most often the PSDs of oceanic particles are measured with a device that is sensitive to the particle's volume (Coulter device). We therefore compare nonspherical particles with spherical particles that have the same volume.

Theoretical considerations suggest that a spherical and a randomly oriented nonspherical particle have the same attenuation in the Rayleigh region, where the particles are small compared with the wavelength.[34] However, for very large particles, in the geometric optics limit, the attenuation of particles is proportional to their cross section, which for convex particles is proportional to their surface area.[35] Since a sphere has the smallest surface area/volume ratio, its attenuation will always be smaller than a nonspherical convex particle with the same volume and index of refraction. This suggests that we may expect differences between the beam-attenuation spectrums of a population of spheres relative to a population of nonspheres. For comparison we use oblates and prolate spheroids with axis ratios of 3 and 1/3, respectively.

The γ–ξ relationship for the nonspherical particles tested here is well described by that of spherical particles. For both types of spheroid, the biggest difference between γ of nonspherical to spherical particles with $n \in \{1.02, 1.05, 1.1, 1.15, 1.2\}$ and $\xi \in \{2.5, 3, 3.5, 4, 4.5, 5\}$ was of 0.03 [a maximum difference of O(18%) in the *magnitude* of the attenuation between the spherical and the nonspherical particles was observed]. Maximum deviation of the attenuation spectrum from a hyperbolic model [Eq. (3)] was equal to that of spheres, 0.2% (rms 0.0002%). We thus conclude that the shape of randomly oriented particles is unlikely to cause large deviations from the conclusions of this paper, as long as the PSD of the nonspherically shaped particles obeys Eq. (1).

3. Discussion

A. Physical Interpretation of Link between the Particle Size Distribution and Spectral Attenuation

Spectral beam attenuation is dependent on size because of the interaction of diffracted rays of light that propagate around the edge of a spherical particle with rays crossing it.[22] The physics of this phenomenon are condensed into a single phase-shift parameter,[22] $\rho = 2\pi|n - 1|D/\lambda$. The position of the maximum volume-specific beam attenuation (beam attenuation normalized by the particle volume) occurs at a similar value of ρ for all particles. At shorter wavelengths, maximum volume-specific beam attenuation will occur for a smaller size of particle than at longer wavelengths [Fig. 6(a)]. Similarly, the larger the index of refraction, the smaller the size of the particle (at a given wavelength) that has the highest volume-specific beam attenuation [Fig. 6(b)]. Absorption effects are important only when a larger number of small absorbing particles will be present [Fig. 6(c)]. The beam-attenuation spectrum of a polydispersion is a convolution of the attenuation response to the particles and the PSD. From the single-particle optical properties outlined above we understand both the sensitivity of the beam-attenuation spectrum to the PSD slope and its dependence on absorption.

A limited range of sizes contributes the most to the beam attenuation [Fig. 6(a)]. Thus the inversion derived here should be applied only to estimate the PSD slope for that size range, namely, for the range of 0.1–30 μm.

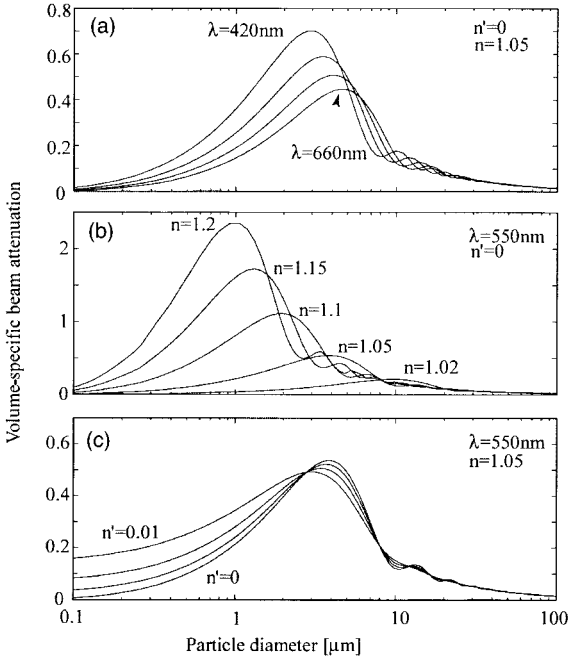

Fig. 6. Volume-specific attenuation coefficient as function of diameter. (a) Changes due to wavelength change (λ = 420, 500, 580, 660 m) for a constant index of refraction, n = 1.05, are displayed in the top panel. (b) Effects due to variation in the real part of the index of refraction (n = 1.02, 1.05, 1.1, 1.15, 1.2), where $n' = 0$ and λ = 550 nm. (c) The effect of absorption (n' = 0, 0.002, 0.005, 0.01) for n = 1.05 and λ = 550 nm.

B. Error Analysis

There are many PSD measurements using Coulter devices, which suggests that the hyperbolic slope changes around particles of 3–8 μm,[1,19] very close to the peak of the particle's volume-specific beam attenuation (Fig. 6). For such a segmented hyperbolic PSD the inversion is likely to provide an estimate of a slope that lies between the two observed slopes. The errors will depend on how different the two slopes of the observations are. It should be noted that there is no consensus on whether this change in

slope in the measured PSD is due to the true PSD or to an instrumental artifact.[21]

In addition, specific groups of algae may occupy a narrow range of sizes in bloom conditions. In such a case the PSD is likely to deviate from hyperbolic and large deviations from Eq. (6) may be expected. For cases in which Eq. (1) still applies, judicious choice of wavelengths with weak absorption to measure attenuation may improve the performance of the inversion (Fig. 5).

Often PSDs depart from a hyperbolic PSD for large particles (>30 μm) because of aggregation processes[36] Such a case is not likely to modify the inversion much for $\xi \geq 3.5$ but may cause a bias for flatter PSDs.

As stated in Section 1, the PSD also depends on the minimum and maximum particle size in the population. In practice, the minimum particulate size is set by a physical filter at the intake of the spectral attenuation meter. For a 0.2-μm prefilter Eq. (6) is still satisfied within 0.15 for $2.5 < \xi < 4$ with deviations increasing to 0.3 for $\xi = 5$ (Fig. 2).

C. Analysis of Other Assumptions

We have assumed, as in previous studies, that the particles, regardless of size, have the same index of refraction. A mixture of particles with different optical properties and sizes may cause deviation from Eq. (6) as well. The bulk index of refraction for such a mixture will be[37]

$$n = \frac{1}{c_p} \sum_i \left[\sum_j c_{\text{ext}}(D_j, n_i) N(D_j, n_i) \right] n_i. \qquad (8)$$

Since the index of refraction may coincide with size, biases in the estimated PSD slope based on Eq. (6) may result. There is just a small body of literature on the distribution of individual oceanic particles and their specific optical and physical properties (exceptions include Stramski and Mobley[23,38]). There is also little knowledge about the PSD and the index of refraction of submicrometer oceanic particles (see Stramski and Kiefer[17], and references therein). This problem is therefore currently unconstrained and will need to be addressed in the future.

Other optical inversion methods exist for obtaining more-detailed PSD information than the single parameter (ξ) sought here.[7,8] The majority of these methods require instrumentation that is not commercially available. An exception is the near-forward-scattering meter[39] (LISST, Sequoia Scientific), which provides an estimate of the PSD for particles spanning from 1.25 to 250 μm. This technology is novel, and we hope to be able to compare and contrast the two inversions in the near future.

4. Summary

We have found in this study that a hyperbolic model [Eq. (3)] provides a robust model for the attenuation spectrum calculated with Mie theory (and T-matrix) regardless of how we perturbed the input variables describing the polydispersed particle population; the worst deviation was found to be O(2%). This suggests that by accurate measurement of the particulate beam attenuation at as little as two wavelengths in the visible it may be possible to extrapolate to other visible wavelengths.

We have modified a model derived in previous investigations that links the shape of the attenuation spectrum and the PSD [Eq. (4)] to incorporate the fact that there is a maximum size for the particles. This model [Eq. (6)] seems adequate even for large perturbations in the assumptions explored here, though departure from the assumptions may be larger in the ocean. The observation that most values of ξ fall near $\xi = 4$ (Refs. 16 and 17) suggest that in most cases Eq. (4) will be a good approximation. The model fails when the PSD is limited to a narrow range of particle sizes, an unlikely situation in the ocean.

When we applied Eq. (6) to a data set comprising 55,000 particulate attenuation spectra collected in July 2000 at the Mid-Atlantic Bight, we found that in 10% of the cases the difference between ξ computed from Eqs. (4) and (6) was bigger than 0.06 and in 5% bigger than 0.14. These larger deviations were associated with resuspended inorganic sediments. These observations as well as those in Boss *et al.*[12] suggest that in most cases Eq. (4) will still be applicable with Eq. (6) providing a significant correction only when large particles are abundant as when sediment resuspension occurs. Equation (6) has the advantage over Eq. (4) in that it is consistent with the measurements of Boss *et al.*[12] (see Fig. 1), which did not observe $\gamma < 0$ even though values ξ as low as 2.4 were measured with a Coulter device.

The recent successes of Barth *et al.*[30] in decomposing the attenuation spectrum and of Boss *et al.*[12] and Twardowski *et al.*[40] in inverting the attenuation spectrum to get the PSD slope testify to the applicability of the hyperbolic shape for particulate attenuation and the possibility of estimating the PSD slope from it. More inquiry into the effect of particle mixtures on the relationship of the beam attenuation and PSD is needed to further delineate the range of conditions in which it is applicable. More observations that relate the PSD slope measured by use of a particle counter with measurements of spectral particulate attenuation are needed for better understanding the range of conditions for application of the model presented here.

The inversion method investigated here provides a single descriptor for the shape of a PSD, namely, the slope of an assumed hyperbolic distribution. If, in certain instances, these relationships are found to be weak predictors of PSD because of the assumptions involved in the proposed inversion, we would expect at least that changes in the slope of the attenuation spectrum within a given water mass could be used to quantify changes in the mean particle size, the first moment of the PSD. For example, in a case of dense

phytoplankton bloom the PSD is likely to deviate significantly from the hyperbolic model, but we would still expect the derived slope to be lower for a bloom of large cells (e.g., diatoms) relative to that of small cells. We strongly recommend that researchers who would like to apply the proposed method in the field concurrently measure the PSD with other methods (e.g., Coulter device) to ascertain the applicability of the underlying assumptions of the inversion investigated here.

Discussions with R. J. V. Zaneveld and W. S. Pegau are greatly acknowledged. Funding for this study was provided by the Environmental Optics Branch of the Office of Naval Research and the ocean biogeochemistry program of NASA.

References

1. J. C. Kitchen, J. R. V. Zaneveld, and H. Pak, "Effect of particle size distribution and chlorophyll content on beam attenuation spectra," Appl. Opt. **21,** 3913–3918 (1982).
2. C. M. Boyd and G. W. Johnson, "Precision of size determination of resistive electronic particle counters," J. Plankton Res. **17,** 41–58 (1995).
3. W. D. Gardner, "Incomplete extraction of rapidly settling particles from water samples," Limnol. Oceanogr. **22,** 764–768 (1977).
4. I. N. McCave, "Particulate size spectra, behavior, and origin of nephloid layers over the Nova Scotian continental rise," J. Geophys. Res. **88,** 7647–7666 (1983).
5. C. Moore, E. J. Bruce, W. S. Pegau, and A. D. Weidemann, "WET Labs ac-9: field calibration protocol, deployment techniques, data processing and design improvements," in *Ocean Optics XIII*, S. G. Ackleson, ed., Proc. SPIE **2963,** 725–730 (1997).
6. G. V. Middleton and J. B. Southard, "Mechanics of sediment movement," SEPM Short Course 3 (Society for Sedimentary Geology, Tulsa, Okla., 1984).
7. K. S. Shifrin, *Physical Optics of Ocean Water* (American Institute of Physics, New York, 1988).
8. K. S. Shifrin and G. Tonna, "Inverse problem related to light scattering in the atmosphere and ocean," in *Advances in Geophysics,* R. Dmowska and B. Saltzman, eds. (Academic, San Diego, Calif., 1993), Vol. 34.
9. F. Volz, "Die Optik und Meterologie der atmospharischen Trubung," Ber. Dtsch. Wetterdienstes **2,** 3–47 (1954).
10. A. Morel, "Diffusion de la lumiere par les eaux de mer. Resultat experimentaux et approch theorique," in Agard Lecture Series 61 on Optics of the Sea (Advisory Group for Aerospace Research and Development; NATO, London, 1973), pp. 3.1.1–76.
11. P. Diehl and H. Haardt, "Measurement of the spectral attenuation to support biological research in a 'plankton tube' experiment," Oceanologica Acta **3,** 89–96 (1980).
12. E. Boss, W. S. Pegau, W. D. Gardner, J. R. V. Zaneveld, A. H. Barnard, M. S. Twardowski, G. C. Chang, and T. D. Dickey, "The spectral particulate attenuation and particle size distribution in the bottom boundary layer of a continental shelf," J. Geophys. Res. **106,** 9509–9516 (2001).
13. K. J. Voss, "A spectral model of the beam attenuation coefficient in the ocean and coastal areas," Limnol. Oceanogr. **37,** 501–509 (1992).
14. A. H. Barnard, W. S. Pegau, and J. R. V. Zaneveld, "Global relationships of the inherent optical properties of the oceans," J. Geophys. Res. **103,** 24955–24968 (1998).
15. G. A. Jackson, R. E. Maffione, D. K. Costello, A. L. Alldredge, B. E. Logan, and H. G. Dam, "Particle size spectra between 1μm and 1cm at Monterey Bay determined using multiple instruments," Deep-Sea Res. **44,** 1739–1768 (1997).
16. H. Bader, "The hyperbolic distribution of particle sizes," J. Geophys. Res. **75,** 2822–2830 (1970).
17. D. Stramski and D. A. Kiefer, "Light scattering by microorganisms in the open ocean," Prog. Oceanogr. **28**, 343–383 (1991).
18. K. J. Voss and R. W. Austin, "Beam-attenuation measurement error due to small-angle scattering," J. Atmos. Ocean. Technol. **10,** 113–121 (1992).
19. M. Jonasz, "Particle size distributions in the Baltic," Tellus Ser. B **35,** 346–358 (1983).
20. D. Risovic, "Two-component model of sea particle size distribution," Deep-Sea Res. **40,** 1459–1473 (1993).
21. I. N. McCave, "Size spectra and aggregation of suspended particles in the deep ocean," Deep-Sea Res. **31,** 329–352 (1984).
22. H. C. van de Hulst, *Light Scattering by Small Particles* (Dover, New York, 1957).
23. D. Stramski and C. D. Mobley, "Effects of microbial particles on oceanic optics: a database of single-particle optical properties," Limnol. Oceanogr. **42,** 538–549 (1997).
24. C. F. Bohren and D. R. Huffman, *Absorption and Scattering of Light by Small Particles* (Wiley, New York, 1983).
25. W. H. Press, S. A. Teukolsky, W. T. Vattering, and B. P. Flannery, *Numerical Recipes in C* (Cambridge U. Press, Cambridge, 1992).
26. G. R. Fournier and T. N. Evans, "Approximation to extinction efficiency for randomly oriented spheroids," Appl. Opt. **30,** 2042–2048 (1991).
27. B. T. N. Evans and G. R. Fournier, "Analytic approximation to randomly oriented spheroid extinction," Appl. Opt. **33,** 5796–5804 (1994).
28. P. C. Waterman, "Matrix methods in potential theory and electromagnetic scattering," J Appl. Phys. **50,** 4550–4566 (1979).
29. M. I. Mishchenko, J. W. Hovenier, and L. D. Travis, *Light Scattering by Nonspherical Particles* (Academic, San Diego, Calif., 2000).
30. H. Barth, K. Grisard, K. Holtsch, R. Reuter, and U. Stute, "Polychromatic transmissometer for *in situ* measurements of suspended particles and gelbstoff in water," Appl. Opt. **36,** 7919–7928 (1997).
31. E. Aas, "Refractive index of phytoplankton derived from its metabolite composition," J. Plankton Res. **18,** 2223–2249 (1996).
32. D. Stramski, A. Morel, and A. Bricaud, "Modeling the light attenuation and scattering by spherical phytoplanktonic cells: a retrieval of the bulk refractive index," Appl. Opt. **27,** 3954–3956 (1988).
33. M. Jonasz, "Nonsphericity of suspended marine particles and its influence on light scattering," Limnol. Ocenaogr. **32,** 1059–1065 (1987).
34. E. Aas, "Influence of shape and structure on light scattering by marine particles," Institute of Geophysics, University of Oslo Rep. 53 (University of Oslo, Oslo, 1984).
35. J. T. O. Kirk, "A theoretical analysis of the contribution of algal cells to the attenuation of light within natural waters," New Phytol. **77,** 341–358 (1976).
36. P. Hill, Department of Oceanography, Dalhousie University, 1355 Oxford Street, Halifax, Nova Scotia B3H 4J1, Canada (personal communication, 2000).

37. J. R. V. Zaneveld, D. M. Roach, and H. Pak, "The determination of the index of refraction distribution of oceanic particulates," J. Geophys. Res. **79,** 4091–4095 (1974).
38. R. Iturriaga and D. A. Siegel, "Microphotometric characterization of phytoplankton and detrital absorption properties in the Sargasso Sea," Limnol. Oceanogr. **34,** 1706–1726 (1989).
39. Y. C. Agrawal and H. C. Pottsmith, "Instruments for particle size and settling velocity observations in sediment transport," Mar. Geol. **168,** 99–114 (2000).
40. M. S. Twardowski, E. Boss, J. B. Macdonald, W. S. Pegau, A. H. Barnard, and J. R. V. Zaneveld, "A model for retrieving oceanic particle composition and size distribution from measurements of the backscattering ratio and spectral attenuation," J. Geophys. Res. (to be published).